DOI: 10.1002/ejic.200600076

Synthesis and Characterization of Ternary $NH_4Ln_2F_7$ (Ln = Y, Ho, Er, Tm, Yb, Lu) Nanocages

Xin Liang,[a] Xun Wang,*[a] Leyu Wang,[a] Ruoxue Yan,[a] Qing Peng,[a] and Yadong Li[a]

Keywords: Nanostructures / Lanthanides

In this paper, a new class of $NH_4Ln_2F_7$ (Ln = Y, Ho, Er, Tm, Yb, Lu) inorganic nanocages that has been discovered will be presented. A facile template-free synthetic route was developed for one step, high yield, and large scale synthesis of ternary $NH_4Ln_2F_7$ (Ln = Y, Ho, Er, Tm, Yb, Lu) nanocages. On the basis of our studies, these nanocages are thermodynamically stable forms of this group of $NH_4Ln_2F_7$ compounds. The tendency of $NH_4Ln_2F_7$ (Ln = Y, Ho, Er, Tm, Yb, Lu) to form these new-type nanostructures is believed to have a close relationship with their inherent layered structures, similar to that of inorganic fullerene-like nanoparticles. This new type of nanocage can be easily doped with other lanthanide ions, which may endow these nanocages with novel properties.

Introduction

In recent years, novel nano-sized morphologies of inorganic materials have become a new focus of research as they may offer new opportunities for application in various areas of nanotechnology, such as optical, biology, and catalysis, etc. Among these different morphologies, hollow nanostructures, as competitive building blocks for future nanodevices, attract considerable interest due to their high surface area and low-density characteristics as well as their other shape-dependent properties.[1–7] Great effort has been focused on the fabrication of different kinds of hollow nanostructures for this is a crucial step in the research and application of hollow nanostructures. Tenne and co-workers successfully synthesized a series of transition metal sulfide fullerene-like hollow nanostructures, such as MoS_2, WS_2, and ReS_2.[8–11] Many other hollow nanostructures (e.g., TiO_2, SnO_2, CdTe) have been prepared by using layer-by-layer self-assembly, sonochemical deposition, chemical-bath deposition, and other template-dependent methods.[12–19] On the basis of the colloidal chemical template-free hydrothermal method, binary lanthanide fluoride and hydroxide fullerene-like hollow spheres have been synthesized.[20] However, to the best of our knowledge, there are few reports concerning a colloidal chemistry-based template-free one-step synthesis of hollow nanostructures with small diameters for ternary (quaternary) lanthanide fluoride compounds. As is well known, MF-LnF_3 is a big family of compounds including many useful materials, such as KY_3F_{10} and $NaYF_4$, which have great potential as biological labels,[21] in solid lasers, and display panels.[22] The tendency of $NH_4Ln_2F_7$ to form these new types of nanostructures is believed to have a close relationship with their inherent layered structures, similar to inorganic fullerene-like nanoparticles. The synthesis of hollow spheres of such complex compounds has great importance and is worthy of thoughtful research.

Herein we report a facile water/ethanol solvothermal synthetic method for one-step, high-yield preparation of a novel family of ternary $NH_4Ln_2F_7$ (Ln = Y, Ho, Er, Tm, Yb, Lu) nanocages under a temperature of 180 °C. The tendency of $NH_4Ln_2F_7$ to form these new types of nanostructures is believed to have a close relationship with their inherent layered structures, similar to inorganic fullerene-like nanoparticles. Since the structures of such materials have great similarity, especially for the KF-LnF_3 and NH_4F-LnF_3 systems, synthesis of other MF-LnF_3 hollow nanostructures should be possible and have great significance.

Results and Discussion

$NH_4Ln_2F_7$ (Ln = Y, Ho, Er, Tm, Yb, Lu) crystallized in a cubic structure. The XRD pattern of $NH_4Y_2F_7$ shown in part a of Figure 1 can be indexed as arising from the pure cubic phase (JCPDS 43-0842) with lattice constant a = 13.4 Å. Similar XRD patterns of a cubic phase were also observed from $NH_4Ho_2F_7$ (JCPDS 43-0842) to $NH_4Lu_2F_7$ (JCPDS 43-0842). The peak positions and relative intensities in those samples were almost identical to those observed in $NH_4Y_2F_7$, which indicated that this class of compounds shares a similar crystal structure. By careful observation a tiny difference can be found in the 2θ values of

[a] Department of Chemistry, Tsinghua University, Beijing 100084, P. R. China
E-mail: wangxun@mail.tsinghua.edu.cn
Supporting information for this article is available on the WWW under http://www.eurjic.org or from the author.

the XRD peaks, which gradually increase on going from $NH_4Ho_2F_7$ to $NH_4Lu_2F_7$, indicating the gradual shrinkage of crystal structures according to the atomic number. The diffraction patterns for $NH_4Ln_2F_7$ (Ln = Y, Ho, Er, Tm, Yb, Lu) group compounds reveal an internal consistency associated with structural isotypes. The work of Krishnan Rajeshwar and Etalo A. Secco et al., showed that the structure of $NH_4Ln_2F_7$ (Ln = Y, Ho, Er, Tm, Yb, Lu) can be visualized as layers of LnF_6 octahedron (built up by mutual sharing of corners and edges) with interleaving layers of NH_4 groups,[23] which is somewhat similar to that of inorganic fullerene-like nanoparticles.

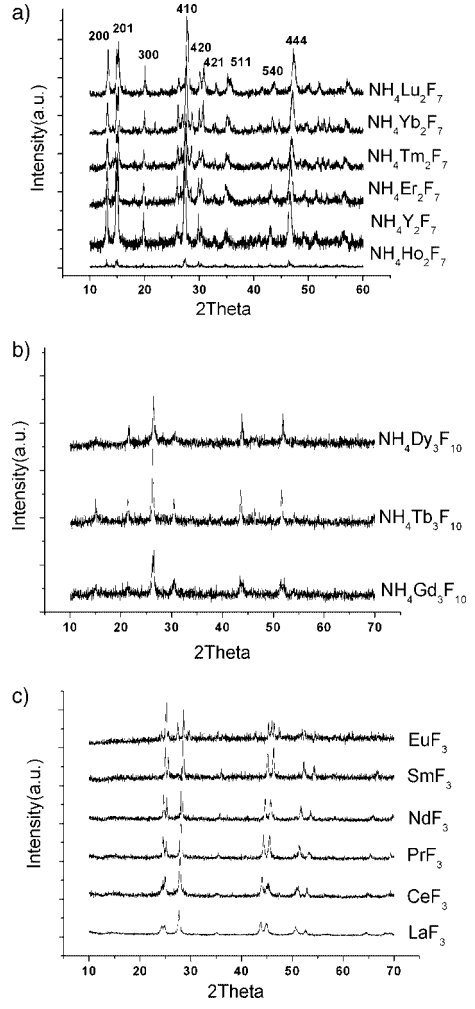

Figure 1. XRD patterns of (a) $NH_4Ln_2F_7$ (Ln = Y, Ho, Er, Tm, Yb, Lu); (b) $NH_4Ln_3F_{10}$ (Ln = Gd, Dy, Tb); (c) LnF_3 (Ln = La–Eu).

On the basis of our former work, we realized that for families of lanthanide compounds that share a similar composition, such as LnF_3[24] and $LnPO_4$,[25] both the crystal structures and physical properties may vary gradually on ascending the series as a result of the lanthanide contraction. For our system, the ionic radii of lanthanide elements were found to be greatly responsible for the phase formation. For all the lanthanide members, the resulting products derived under the same synthetic conditions were of different structure. The variation in the structure is believed to be caused by the contraction of ionic radii of Ln^{3+} (Table 1). The members from Lu to Ho, ionic radius 0.85–0.89 Å, formed $NH_4Ln_2F_7$ compounds; the members from La to Dy, whose ionic radii range 1.06–0.91 Å, adopt other crystal structures that are different from the layered structures of $NH_4Ln_2F_7$. The XRD patterns of other lanthanide categories from La–Dy can be seen in Figure 1 (parts b, c). For the larger lanthanide ions (Ln = La, Ce, Nd, Pr, Sm, Eu), LnF_3 structures were obtained (Ln = La–Sm, the resulting products are pure hexagonal structures; Ln = Eu, a mixture of hexagonal and orthorhombic structures were found). For the intermediate-sized lanthanide ions (Ln = Gd, Tb, Dy) $NH_4Ln_3F_{10}$ was formed.[26]

The morphology and microstructural details can be observed from the TEM, HRTEM observations. The typical low-magnification images of the as-prepared $NH_4Ln_2F_7$ (Ln = Y, Ho, Er, Tm, Yb, Lu) nanocages (here Y, Ho, and Tm have been chosen as examples) are shown in Figure 2. The hollow interior features of $NH_4Ln_2F_7$ nanocages were confirmed by the TEM observations. It can be seen from Figure 2 (a–c) that nearly all the nanoparticles in the images are of hollow interiors and the nanoparticles are uniform with an average size of 20–30 nm. Careful TEM observations were also carried out on both the LnF_3 (Ln = La–Eu) and $NH_4Ln_3F_{10}$ (Ln = Gd–Dy) series (TEM images are found in the supporting information). However, only a few hollow-sphere-type structures were found. This morphology difference between $NH_4Ln_2F_7$ (Ln = Y, Ho, Er, Tm, Yb, Lu), LnF_3 (Ln = La–Eu), and $NH_4Ln_3F_{10}$ (Ln = Gd–Dy) indicates that the formation of the hollow interior forms is unique to the $NH_4Ln_2F_7$ series and it also excludes the possibility that the nanocages were formed by the Marangoni effect. That is where the concentrated solutes diffuse out into the droplet-vapor interface leaving the pure solvent behind in the center of the nanoparticle. At this point the solvent evaporates leaving the polycrystalline material to deposit on the outer circumference and leaving a hollow core in the center. According to this assumption, nanocages

Table 1. Crystal structure and chemical composition of lanthanide compounds obtained under the identical synthetic condition (h&o is short for hexagonal and orthorhombic).

Ln^{3+}	La	Ce	Nd	Pr	Sm	Eu	Gd	Tb	Dy	Ho	Y	Er	Tm	Yb	Lu
R(Ln^{3+}) [Å]	1.06	1.03	1.01	1.00	0.96	0.95	0.94	0.92	0.91	0.89	0.89	0.88	0.87	0.86	0.85
Products	LnF_3						$NH_4Ln_3F_{10}$			$NH_4Ln_2F_7$					
Crystal structures	hexagonal					h&o	cubic			cubic					

would form in other lanthanide categories from La to Dy, because of the similar environments in the growth procedure.

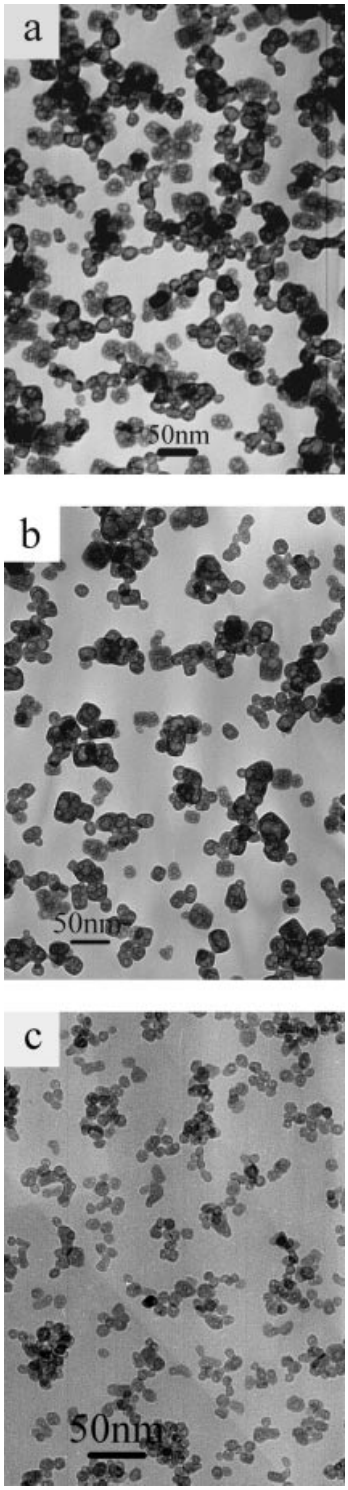

Figure 2. TEM images of (a) $NH_4Y_2F_7$ nanocages; (b) $NH_4Tm_2F_7$ nanocages; (c) the Tem images of $NH_4Ho_2F_7$ nanocages.

HRTEM characterization (Figure 3, a–f) provides us with further insight into the structural details of $NH_4Ln_2F_7$ nanocages. It can be seen from the HRTEM images that most of the nanoparticles usually had a hollow interior, which proved the formation of hollow sphere nanostructures under current experimental conditions. The distance between the inner and outer layers was calculated to be approximately 0.32 nm for $NH_4Y_2F_7$ nanocages, corresponding to the crystal plane of (410), and the other categories show a close value of about 0.32 nm, indicating a similar formation mode under adopted conditions. Though the crystal lattices were somewhat distorted compared with the typical onion-like lattices of fullerene-like nanoparticles, the lattice striations displayed a nearly close-caged configuration with high crystallinity. The electronic diffraction of the selected area (insert in Figure 3, a), where the diffractive dots of single crystal can be clearly seen, further confirmed the single crystal features of the nanocages. It is interesting to note that the inner spaces are usually quite different in shape, including all kinds of irregular polygons, indicating that the growth of these structures might be rather sensitive to fluctuations from the outer environment. Nevertheless, the nanoparticles with hollow interiors can be easily obtained under designed synthetic conditions, and from the TEM images we can see that almost all of the final products are hollow nanostructures. The HRTEM observations confirmed that the formation of the nanocages may have a close relationship with the inherent layered structure of $NH_4Ln_2F_7$.

The thermal gravimetric analysis was carried out to study the thermal stability of these nanocages. $NH_4Ln_2F_7$ (Ln = Y, Ho, Er, Tm, Yb, Lu) decomposes at high temperature. The TGA curves for $NH_4Ln_2F_7$ (Ln = Y, Ho, Tm) powders are shown in Figure 4. From the TGA curves, two weight-loss steps can be observed. The first step is from room temperature to 250 °C, in which, the mild weight loss may be caused by desorption of water and other solvents such as ethanol on the $NH_4Ln_2F_7$ surface. The main weight loss occurs in the temperature range from 250 to 360 °C. In this step, $NH_4Ln_2F_7$ converted to LnF_3. The experimental weight loss is about 11.10 wt.-% for $NH_4Y_2F_7$, 7.35 wt.-% for $NH_4Ho_2F_7$, and 6.84 wt.-% for $NH_4Tm_2F_7$, respectively, which agrees well with the theoretical weight loss of the decomposition of $NH_4Ln_2F_7$ to LnF_3 (11.25 wt.-% for $NH_4Y_2F_7$, 7.69 wt.-% for $NH_4Ho_2F_7$, and 7.57 wt.-% for $NH_4Tm_2F_7$). The chemical reaction that occurs in the process of this main weight loss can be expressed as follows:

$$NH_4Ln_2F_7 \rightarrow LnF_3 + NH_3 \uparrow + HF \uparrow$$

The decomposition temperature of these three samples is quite similar. It is about 356 °C for $NH_4Y_2F_7$, 352 °C for $NH_4Ho_2F_7$, and 361 °C for $NH_4Tm_2F_7$.

$NH_4Y_2F_7$ samples were annealed at 200 and 400 °C for 3 h to investigate this conversion process. XRD confirmed that the sample annealed at 200 °C remained as $NH_4Y_2F_7$; in contrast the sample annealed at 400 °C converted to YF_3 completely. TEM images of the samples derived at different annealing temperatures are shown in Figure 5 from which we can see that most of the $NH_4Y_2F_7$ nanoparticles remain intact with hollow interiors and have no apparent aggregation after being annealed at 200 °C for 3 h, in contrast to the nanoparticles annealed at 400 °C that have aggregated

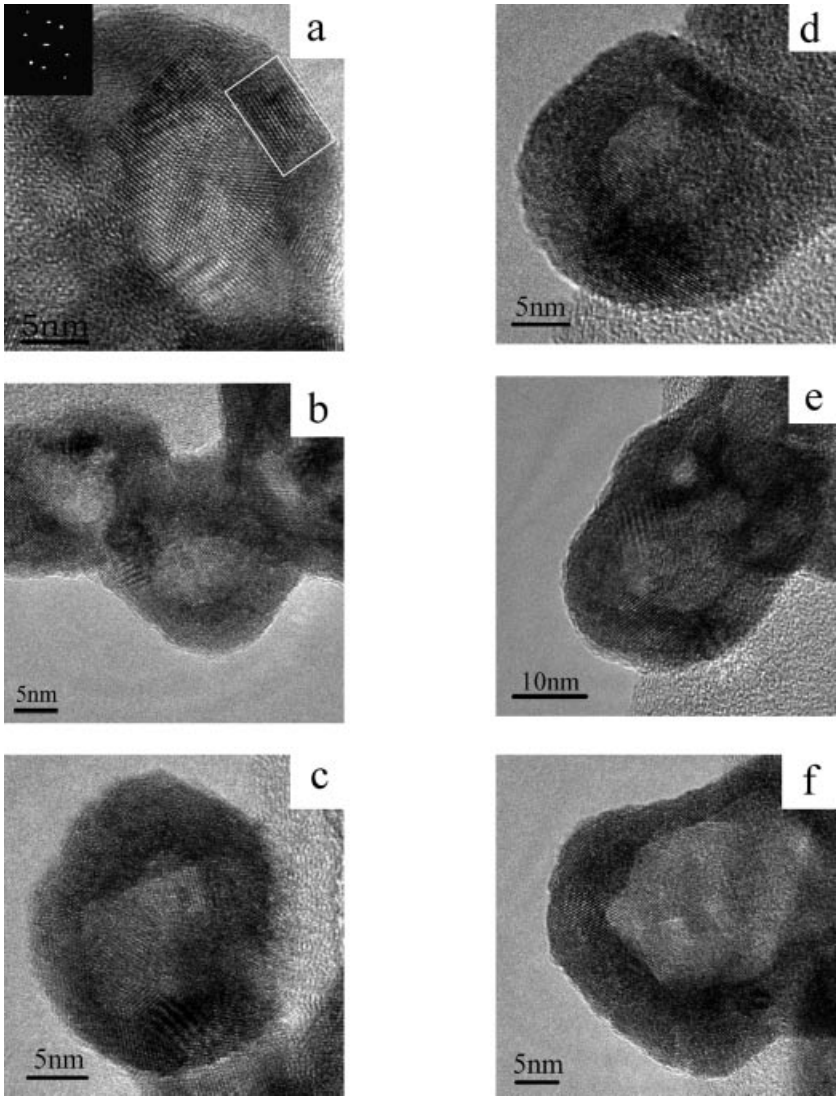

Figure 3. HRTEM image of (a) an individual $NH_4Y_2F_7$ nanocage with diameter about 22 nm, the inset is an EDS analysis of the selected area; (b) three conterminous $NH_4Y_2F_7$ nanocages; (c) an individual $NH_4Y_2F_7$ nanocage with diameter ca. 20 nm; (d) an individual globular $NH_4Tm_2F_7$ nanocage; (e) an individual $NH_4Yb_2F_7$ nanocage; (f) $NH_4Ho_2F_7$ nanocage.

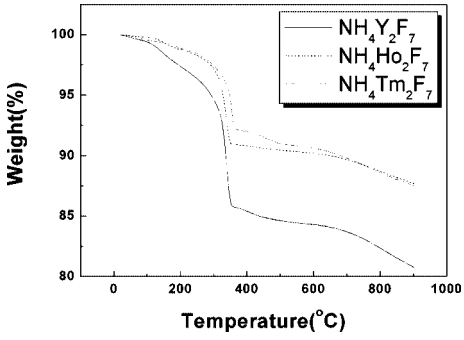

Figure 4. TGA curves of $NH_4Ln_2F_7$ (Ln = Y, Ho, Tm).

to a large extent with no remaining nanocages. These results show that the nanocages can be maintained at the relatively high temperature of 200 °C before the composition of $NH_4Y_2F_7$ and the hollow interior forms collapse as $NH_4Y_2F_7$ converts to YF_3 at higher temperature. As the literature has reported, the structure of $NH_4Y_2F_7$ can be visualized as layers of YF_6 octahedron with interleaving layers of NH_4 groups and the hydrogen bonding effect of NH_4^+ is a critical factor responsible for the stability of ammonium fluorometallates.[27–28] The layered structure of $NH_4Y_2F_7$ would collapse if the interleaving layers of NH_4 groups were lost. So it is believed that ammonium loss in the process of conversion of $NH_4Y_2F_7$ to YF_3 is an important factor in the collapse of the nanocages. These phenomena show that the inner structure of $NH_4Y_2F_7$ is very important for the stability of these hollow interior forms.

Y^{3+}, Ho^{3+}, Er^{3+}, Tm^{3+}, Yb^{3+}, and Lu^{3+} can crystallize in homogeneous phase $NH_4Ln_2F_7$ and their ionic radii are similar, thus making it convenient to dope $NH_4Ln_2F_7$ nanocages with these lanthanide ions, which may then endow this class of nanocage with novel properties. The most frequently used up-conversion ion Er^{3+} and the sensitizer ion

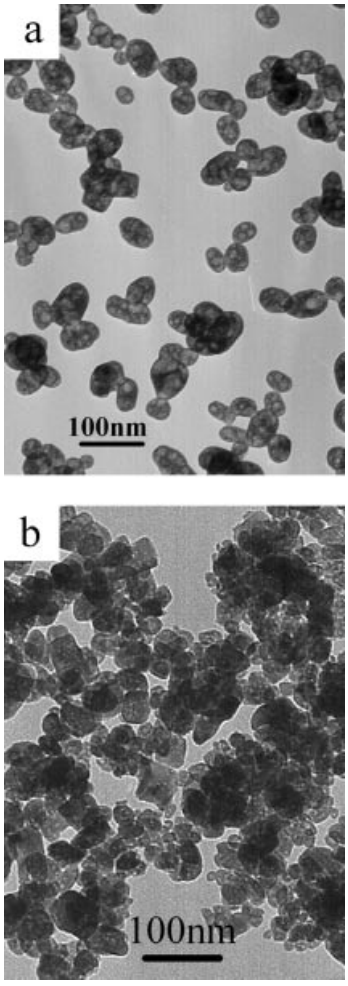

Figure 5. TEM images of samples annealed at (a) 200 °C; (b) 400 °C.

Yb^{3+} were co-doped into $NH_4Y_2F_7$ to denote the feasibility of doping lanthanide ions into $NH_4Ln_2F_7$. Doped samples were prepared by the same synthetic procedure, except for adding 5% (total molar ration) $YbCl_3$ and $ErCl_3$ in YCl_3 in the first stage. The up-conversion fluorescence property of the final product was measured by a 980-nm IR laser. The up-conversion emission of doped $NH_4Y_2F_7$ sample is weak due to the quenching effect of ammonium. After being annealed at 500 °C for 3 h, the $NH_4Y_2F_7$ can convert into

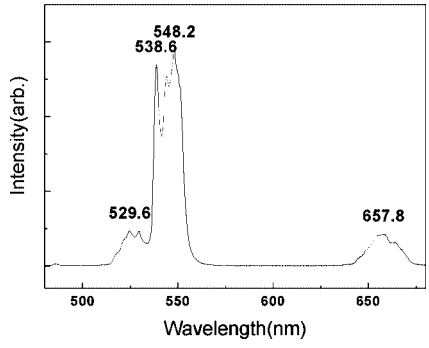

Figure 6. UC emission spectra of YF_3 (Er^{3+}, Yb^{3+}).

YF_3 (revealed by the XRD analysis). It can be seen that the up-conversion emission is stronger and can be observed by the naked eye. The UC spectrum exhibits the characteristic peaks of an Er^{3+}- and Yb^{3+}-doped YF_3 system (Figure 6). This consequence proves the successful doping of Er^{3+}/Yb^{3+} into $NH_4Y_2F_7$.

Conclusion

In this work, a novel class of ammonium lanthanide fluoride nanocage was successfully synthesized. The tendency of $NH_4Ln_2F_7$ to form nanocages is believed to have a close relationship with their inner structure. Our study presents the first example of ternary nanocages to the best of our knowledge. We believe that this method could be expanded to the synthesis of other rare-earth hollow nanostructures, especially the MF-LnF_3 categories, and thus brings new opportunities to these fast expanding research fields.

Experimental Section

In a general preparation, EDTA chelated with Ln^{3+} to form a clear solution at pH 2–3 by adding diluted HCl and $NH_3{\cdot}H_2O$ solution. And then NH_4F, which was dissolved into water/ethanol mixed solvents, was added. The mixture was transferred to an autoclave and was treated at 180 °C for 20 h under solvothermal conditions. The autoclave was then cooled to room temperature. The precipitate was then filtered, washed with water to remove ions possibly remnant in the final products, and dried at 80 °C in air. Following the above procedures, $NH_4Ln_2F_7$ (Ln = Y, Ho, Er, Tm, Yb, Lu) nanocages with high yield (90%) could be obtained.

NH_4^+ and EDTA are found to be responsible for the phase formation of $NH_4Y_2F_7$. To investigate the influence of NH_4^+, EDTA was dissolved with NaOH instead of $NH_3{\cdot}H_2O$, and then $NaYF_4$ was prepared and no hollow-sphere structures were found in the samples. This result confirms that it is easy to induce other cations to take the place of ammonium in the products. The concentration of EDTA greatly affects the phase purity of $NH_4Y_2F_7$. Keeping the amount of Y^{3+} (0.2 mmol) unchanged, when the amount of EDTA is less than 0.2 g, the resulting products are mixtures of flakes and hollow-spheres. When the amount of EDTA is more than 1.0 g, the nanocages were elongated to an irregular form. Similar phenomena have been observed on the samples of other $NH_4Ln_2F_7$ (Ln = Ho, Er, Tm, Yb, Lu). When the amount of EDTA is kept at 0.2–1.0 g, regular nanocages can be easily obtained on a large scale.

The obtained sample was characterized by a Bruker D8-Advance X-ray powder diffractometer with Cu-K_a radiation (λ = 1.5418 Å). The size and morphology of the IF nanoparticles were determined at 200 kV by a Hitachi H-800 transmission electron microscope (TEM) and a JEOL JEM-2010F high-resolution transmission electron microscope. Fluorescent spectra were recorded with a Hitachi F-4500 Fluorescence Spectrophotometer. Up-conversion fluorescent spectra were obtained with the LS-50B fluorescence spectrophotometer (Perkin–Elmer Corp., Forster City, CA) with an external 0–800 mW adjustable laser (980 nm, Beijing Hi-Tech Optoelectronic Co., China) as the excitation source, instead of the Xenon source in the spectrophotometer, and with an optic fiber accessory. The thermal decomposition behavior of the $NH_4Ln_2F_7$ (Ln = Y, Ho, Tm) samples was studied by thermogravimetric analysis (TGA) with a TGA2050 thermal analysis device (American TA Corpora-

tion). TGA determination was carried out in nitrogen at a heating rate of 20 °C/min in a range of room temperature to 900 °C.

Supporting Information (for details see the footnote on the first page of this article): XRD patterns of samples that were annealed at 200 °C and 400 °C, respectively, and the TEM images of CeF_3, SmF_3, and $NH_4Tb_3F_{10}$.

Acknowledgments

This work was supported by NSFC (20501013, 50372030, 20131030, 90406003), the Foundation for the Author of National Excellent Doctoral Dissertation of P. R. China and the State Key Project of Fundamental Research for Nanomaterials and Nanostructures (2003CB716901).

[1] Y. N. Xia, B. Gates, Y. D. Yin, Y. Lu, *Adv. Mater.* **2000**, *12*, 693–713.
[2] M. Prato, M. Maggini, *Acc. Chem. Res.* **1998**, *31*, 519–526.
[3] A. L. Balch, M. M. Olmstead, *Chem. Rev.* **1998**, *98*, 2123–2165.
[4] F. Caruso, R. A. Caruso, H. Möhwald, *Science* **1998**, *282*, 1111–1114.
[5] C. G. Göltner, *Angew. Chem. Int. Ed.* **1999**, *38*, 3155–3156.
[6] Y. G. Sun, Y. N. Xia, *Science* **2002**, *298*, 2176–2179.
[7] Y. G. Sun, B. Mayers, Y. N. Xia, *Adv. Mater.* **2003**, *15*, 641–646.
[8] R. Tenne, L. Margulis, M. Genut, G. Hodes, *Nature* **1992**, *360*, 444–446.
[9] L. Margulis, G. Salitra, R. Tenne, M. Talianker, *Nature* **1993**, *365*, 113–114.
[10] Y. Feldman, E. Wasserman, D. A. Srolovitz, R. Tenne, *Science* **1995**, *267*, 222–225.
[11] Y. R. Hacohen, E. Grunbaum, R. Tenne, J. Sloan, J. L. Hutchison, *Nature* **1998**, *395*, 336–337.
[12] T. Nakashima, N. Kimizuka, *J. Am. Chem. Soc.* **2003**, *125*, 6386–6387.
[13] N. A. Dhas, K. S. Suslick, *J. Am. Chem. Soc.* **2005**, *127*, 2368–2369.
[14] X. M. Sun, Y. D. Li, *Angew. Chem. Int. Ed.* **2004**, *43*, 3827–3831.
[15] P. Selvakannan, M. Sastry, *Chem. Commun.* **2005**, 1684–1686.
[16] H. Liang, Y. Guo, H. Zhang, J. Hu, L. Wan, C. Bai, *Chem. Commun.* **2004**, 1496–1497.
[17] S. Lei, K. Tang, Q. Yang, H. Zheng, *Eur. J. Inorg. Chem.* **2005**, *20*, 4124–4128.
[18] S. Xu, H. Wang, J. J. Zhu, X. Q. Xin, H. Y. Chen, *Eur. J. Inorg. Chem.* **2004**, *23*, 4653–4659.
[19] G. Zou, Z. P. Liu, D. B. Wang, C. L. Jiang, Y. T. Qian, *Eur. J. Inorg. Chem.* **2004**, *22*, 4521–4524.
[20] X. Wang, Y. D. Li, *Angew. Chem. Int. Ed.* **2003**, *42*, 3497–3500.
[21] L. Y. Wang, R. X. Yan, Z. Y. Huo, L. Wang, J. Z. Hui, J. Bao, X. Wang, Q. Peng, Y. D. Li, *Angew. Chem. Int. Ed.* **2005**, *44*, 6054–6057.
[22] J. H. Zeng, J. Su, Z. H. Li, R. X. Yan, Y. D. Li, *Adv. Mater.* **2005**, *17*, 2119–2123.
[23] K. Rajeshwar, E. A. Secco, *Can. J. Chem.* **1977**, *55*, 2620–2627.
[24] a) X. Wang, Y. D. Li, *Chem. Eur. J.* **2003**, *9*, 5627–5635; b) X. Wang, X. M. Sun, D. P. Yu, B. S. Zhou, Y. D. Li, *Adv. Mater.* **2003**, *15*, 1442–1445.
[25] R. X. Yan, X. M. Sun, X. Wang, Q. Peng, Y. D. Li, *Chem. Eur. J.* **2005**, *11*, 2183–2195.
[26] Z. J. Kang, Y. X. Wang, F. T. You, J. H. Lin, *J. Solid State Chem.* **2001**, *158*, 358–362.
[27] R. E. Thoma, *Inorg. Chem.* **1962**, *1*, 220–226.
[28] A. Tressaud, J. Portier, R. Depage, P. Hagenmuller, *J. Solid State Chem.* **1970**, *2*, 269–275.

Received: January 25, 2006
Published Online: March 31, 2006

